Asian Journal of Water, Environment and Pollution. Vol. 22, No. 4 (2025), pp. 205-218.
doi: 10.36922/AJWEP025240193

ORIGINAL RESEARCH ARTICLE

Porosity-driven combustion behavior in fluffy biomass waste: Toward safer and smarter energy utilization

Zhiyuan Ma, Zhuoying Chen, Qingchun Wang, Xiangyue Yuan*, and Zhongjia Chen

Biomass Laboratory, School of Technology, Beijing Forestry University, Beijing, China
***Corresponding author:** Xiangyue Yuan (yuanxiangyue@bjfu.edu.cn)

Received: June 10, 2025; 1st revised: July 4, 2025; 2nd revised: July 9, 2025; Accepted: July 10, 2025; Published online: July 31, 2025

Abstract: Biomass fractions within municipal solid waste present significant fire hazards and environmental pollution risks, amplified by their distinct physical architectures. Discarded cotton wadding and poplar fluff, characterized by porous, fluffy morphologies and high specific surface areas, readily form combustible air-premixed systems during storage and transport, posing risks of uncontrolled fires and associated pollutant release. Understanding the combustion kinetics of such waste streams is critical not only for fire safety but also for assessing their potential for efficient energy conversion and minimizing incomplete combustion emissions. This study focused on a representative elongated fibrous biomass: waste cotton floc. By integrating microscopic structural characterization with theoretical combustion modeling, we systematically uncovered the unique deflagration behavior and latent hazards associated with this class of materials, linking them to potential environmental impacts. A custom setup with high-speed imaging quantified flame spread (1.5 m/s in confined conditions vs. 0.8 m/s in open conditions) and reaction times. Confined burning, which mimics common waste accumulation scenarios, such as containers or piles, displayed 85% faster propagation but lower combustion efficiency (stabilizing at ~20% with higher fuel loads) and ultra-short combustion durations (0.2 s at peak loading); these conditions favor incomplete combustion and elevated pollutant generation. The proposed structural fuel theory identified porosity as the key control parameter, linking fiber network topology to combustion dynamics and pollutant formation potential. These insights are vital for advancing strategies to mitigate combustion-related pollution events, optimize waste biomass energy recovery efficiency, and enhance fire safety protocols within the waste management sector to protect environmental quality.

Keywords: Biomass waste; Biomass energy; Long fibers; Porosity; Deflagration

1. Introduction

The unsustainable exploitation of fossil fuels accelerates resource depletion and intensifies climate change through greenhouse gas emissions and persistent pollutant accumulation.[1] As a promising alternative, bioenergy systems enable solar energy to be stored in biomass through photosynthesis and subsequently transformed into liquid biofuels, solid biochar, and gaseous biogas through thermochemical or biochemical pathways.[2-4] Such systems are critical to supporting global decarbonization efforts[3] and may enable transitions to carbon-negative power systems when integrated with carbon capture and storage technologies.[2]

Biomass, especially from forestry and agricultural residues, has considerable global potential for renewable energy production,[5] with liquid biofuels gaining strategic importance in Europe and other regions. Global bioenergy output was approximately 40 EJ in 2023, covering about 5% of primary energy demand, and it is expected to reach 100 EJ by 2050, potentially replacing up to 27% of transport fuels.[6-8] In China, multi-source biomass resources equivalent to 460 million tons of standard coal are available annually,[9] and Figure 1 illustrates the status of biomass energy conversion and overall resource availability as of 2020. Bibliometric analyses confirm that biomass research is increasingly focused on improving conversion efficiency and safety.[6]

A critical challenge in biomass utilization is the control of combustion processes, especially for dust fuels, which are characterized by high surface area and reactivity.[10] Huang[10] derived predictive formulas to evaluate the minimum ignition temperature and energy of wood-plastic composite dust, emphasizing the strong effect of concentration on deflagration sensitivity. Zhang *et al*.[11] compared the pyrolysis and explosion behavior of rosewood and poplar fiber dust, revealing a higher explosion risk for rosewood due to lower activation energy. Jiang *et al.*[12] characterized distillers dried grains with solubles dust as St1 (low hazard) and determined its ignition parameters. Zhang *et al*.[13] observed spiral flame propagation in corn starch dust explosions at different airflow velocities, while Zhang *et al*.[14] clarified the effects of ignition energy on the explosion limits of tapioca starch.

Chen[15] and Liu *et al*.[16] indicated that cellulose content increases maximum explosion pressure, whereas higher lignin reduces it. Lv *et al*.[17] confirmed that smaller particle sizes release more energy. Wang *et al*.[18] reviewed minimum ignition energy tests, analyzing dispersion and static electricity influences. Zhang and Zhou[19] found that the ignition temperature of bamboo dust initially decreases with concentration and then stabilizes. Wu *et al*.[20] highlighted the impacts of volatile content and ash on oil shale dust explosions.

He *et al*.[21] identified tobacco dust explosions as most severe in extraction pipes. Yang *et al*.[22] demonstrated that a smaller particle size in lutein residue dusts leads to lower explosion limit concentration and higher peak pressure. Islas *et al*.[23,24] simulated biomass dust explosions, revealing the critical role of venting systems. Medina *et al*.[25] and Slatter *et al*.[26] revealed comparable or higher explosion hazards of biomass dust relative to coal.

Recent advances in biomass pyrolysis and flame dynamics were reported by Shen *et al*.,[27] Liu *et al*.,[28] and Wen *et al*.,[29] while Yang *et al*.[30] confirmed explosibility in biomass fuel mixtures. Liu *et al*.[31] analyzed kinetic degradation during volatile combustion and diffusion during char combustion. Mulky and Niemeyer[32] modeled smoldering behavior in cellulose-hemicellulose mixtures, clarifying the effects of fuel composition and moisture.

Recent studies have demonstrated that the combustion and explosion behaviors of biomass dust are significantly influenced by particle morphology, pore structure, and chemical composition.[10-22] However, most existing research focuses primarily on homogeneous biomass dusts or simple fibrous systems, such as wood dust, bamboo dust, and straw particles,[11,12,19] without adequately considering the multiscale pore architectures present in actual waste materials.[27-32] Moreover, systematic investigations into the coupling effects of pore distribution on flame propagation dynamics and reaction time remain limited. Addressing these gaps is critical for developing accurate fire risk assessments and safety strategies for biomass-derived wastes.

This study aims to investigate the energy utilization of long-fiber biomass materials by establishing the relationship between input quantity, reaction time, and efficiency. By optimizing reaction conditions and enhancing resource utilization, the study provides a theoretical foundation for equipment design and process refinement. In addition, this study fills a gap in biomass combustion research by developing a fire safety assessment model tailored to heterogeneous biomass. It is the first to focus on the multiscale pore architecture of waste cotton flocs – contrasting with conventional studies on homogeneous dust or straw systems – unveiling new mechanisms by which pore

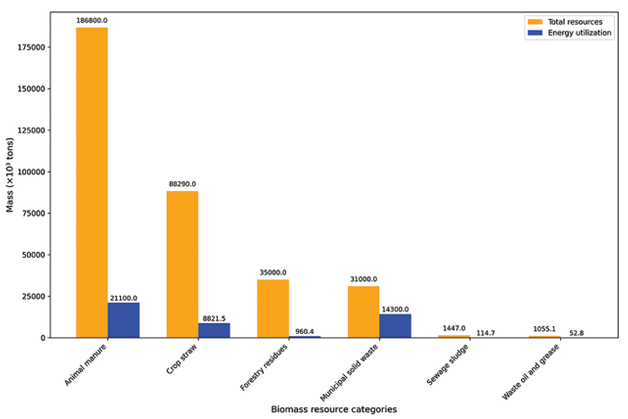

Figure 1. Current status of biomass resources and energy utilization in China

distribution regulates flame propagation and reaction time. This work advances the paradigm shift in solid waste management from passive disposal toward proactive prevention, energy recovery, and carbon reduction integration. Future research should extend to other highly porous wastes, such as plastic foam and textile fragments, aiming to establish a universal urban solid waste combustion and pollution prediction model.

1.1. Characteristics of deflagration in elongated fibrous biomass materials

Elongated fibrous biomass materials, such as cotton, pose high safety risks during deflagration, primarily due to their physical structure, chemical properties, and environmental conditions. Their characteristics are as follows:

(i) High flammability: Elongated fibers, characterized by their loose structure and high specific surface area, readily adsorb atmospheric oxygen, ensuring an ample oxidizer supply for combustion. Their elevated volatile content and low ignition temperature (~250°C) render them highly susceptible to ignition from sparks, static discharge, or elevated temperatures. These properties facilitate rapid combustion propagation, increasing the risk of deflagration, localized pressure surges, and severe safety hazards. Consequently, stringent fire prevention and anti-static measures are imperative across storage, transportation, and operational phases to mitigate fire and explosion risks.

(ii) Rapid deflagration propagation: Fibrous materials, when suspended, readily form floc-like clouds that mix with air to generate combustible aerosols. Upon ignition, these mixtures undergo rapid combustion, releasing substantial heat and gaseous byproducts, thereby triggering intense deflagration. This process induces localized high-temperature and high-pressure conditions, posing severe risks to equipment integrity and personnel safety. The propagation of deflagration may initiate chain reactions, endangering storage facilities, transportation pipelines, and adjacent infrastructure, thereby amplifying potential damage. To mitigate these hazards, stringent control over fiber-air mixing, reinforced fire prevention and anti-static measures, as well as optimized ventilation and explosion relief designs, are critical.

(iii) Risk of electrostatic ignition: During processing, transportation, and storage, fibrous materials generate static electricity through friction with equipment or pipeline surfaces. Due to their loose structure, charge dissipation is hindered, leading to gradual accumulation and potential electrostatic discharge. Such discharges can generate sparks, igniting nearby combustibles and triggering fires or deflagrations, with the risk further exacerbated in low-humidity environments. To mitigate these hazards, preventive measures – including equipment grounding, incorporation of conductive materials, humidity control, and enhanced monitoring of high-risk zones – are essential for reducing static-induced fire risks.

(iv) Combustion enhancement in high-temperature environments: Under high-temperature conditions, fibrous materials undergo pyrolysis, releasing volatil2 combustible gases and elevating combustion risks. Prolonged exposure can lead to heat accumulation, potentially triggering spontaneous combustion even in the absence of an open flame. Elevated temperatures further accelerate pyrolysis, compounding fire hazards. To mitigate these risks, stringent temperature monitoring, optimized ventilation management, and strict avoidance of heat sources are critical. In addition, flame-retardant treatments and thermal insulation measures are essential to reduce fire and spontaneous combustion hazards, ensuring fundamental safety in storage and operation.

1.2. Fundamental principles of deflagration in elongated fibrous biomass materials

Biomass deflagration is a complex chemical reaction process involving the rapid decomposition, oxidation, and combustion of fuel molecules under high-temperature conditions.[33] The main reaction processes and energy release are as follows:

(i) Pyrolysis stage: Under high temperatures, biomass initially decomposes into gases (such as H_2, CH_4, and CO), tar, and solid carbon residues (biochar). This stage does not require oxygen but generates a significant amount of volatile gases, providing reactants for subsequent oxidation.[34]

(ii) Oxidation stage: In the presence of oxygen, volatile gases undergo rapid oxidation and combustion, releasing substantial heat. This process is fundamental to deflagration, as the rapid oxidation of gaseous species results in instantaneous heat release, generating a high-energy deflagration effect.

(iii) Char combustion stage: Following the combustion of volatile gases, the residual biochar undergoes gradual oxidation, generating CO_2 and trace amounts

of CO. Although this process releases comparatively less energy, it sustains combustion over an extended duration, contributing to prolonged heat output.

Biomass materials undergo complex chemical reactions in the three stages above, releasing a significant amount of heat. Particularly in the oxidation stage, the heat is released instantaneously, making it highly susceptible to deflagration.

1.3. Deflagration process

The deflagration process of cotton floc can be analyzed using experimental data obtained from pipeline testing and high-speed camera recordings of the complete combustion process.[35-38]

Pipeline testing is a well-established method for measuring flame propagation speed in gas mixtures, particularly in industrial combustion and safety studies. The experimental setup primarily consists of a high-speed camera, a 100 mm diameter, 200 mm long pipeline, and a high-voltage electric spark generator, as illustrated in Figure 2.

2. Materials and methods

2.1. Materials

The cotton floc samples were obtained from Xinjiang Province in northern China. The cotton floc samples exhibited a moisture content of approximately 3%, a bulk density of 0.12 – 0.16 g/cm^3 in the loosely packed state, and fiber morphological parameters, including lengths of 28 – 36 mm and diameters of approximately 20 μm. The true density, corresponding to cellulose density, was measured as 1.54 g/cm^3. Before experimentation, the flocs were mechanically processed by cutting into shorter segments and aerodynamically disentangled to ensure structural uniformity.

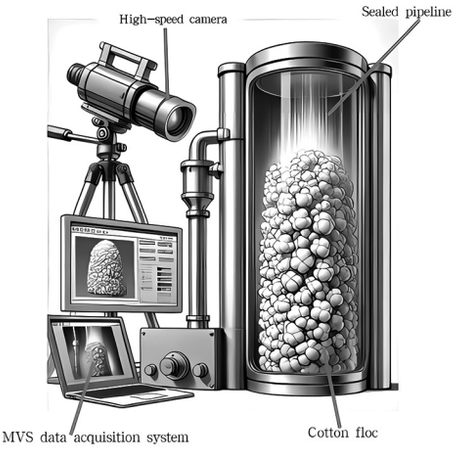

Figure 2. Schematic diagram of the pipeline test apparatus

Abbreviation: MVS: Machine Vision Software.

2.2. Deflagration test

The deflagration test apparatus comprises a 1 L reaction chamber, a high-voltage spark igniter (0.5 kV), a high-speed industrial area-array camera (100 frames/s) for observing flame morphology and combustion pressure, a halogen moisture analyzer for measuring the moisture content of biomass materials, an electronic balance (precision of 0.0001 g), a Machine Vision Software data acquisition system, and an experimental rack (Figure 3).

For the deflagration test, the required amount of cotton floc was first weighed using an electronic balance, and the weight was recorded before placing the cotton floc at the bottom of the reaction chamber. The equipment power was turned on, and the high-voltage igniter was activated by the timer controller to ignite the cotton floc inside the reaction chamber. The combustion process was recorded using a high-speed camera, while the details were simultaneously captured by the data acquisition system. After the reaction was complete, the ignition was stopped, and the power to all equipment was turned off. The remaining biomass after the reaction was removed and weighed using the balance. The biomass utilization rate was then calculated according to Equation I:

$$Utilization\ rate = \left(1 - \frac{Residual\ mass}{Input\ mass}\right) \times 100\% \qquad (I)$$

2.3. Experimental procedure

1. Weigh the required amount of cotton fluff using an electronic balance and record the weight, then place it at the bottom of the reaction chamber
2. Turn on the equipment power and use the timer controller to activate the high-voltage igniter to ignite the cotton fluff inside the reaction chamber
3. Use a high-speed camera to record the combustion process while simultaneously using the data acquisition system to record the details
4. After the reaction is complete, stop the ignition and turn off the power to all equipment
5. Remove the remaining biomass after the reaction and weigh it using the balance. Then, calculate the biomass utilization rate according to Equation I.

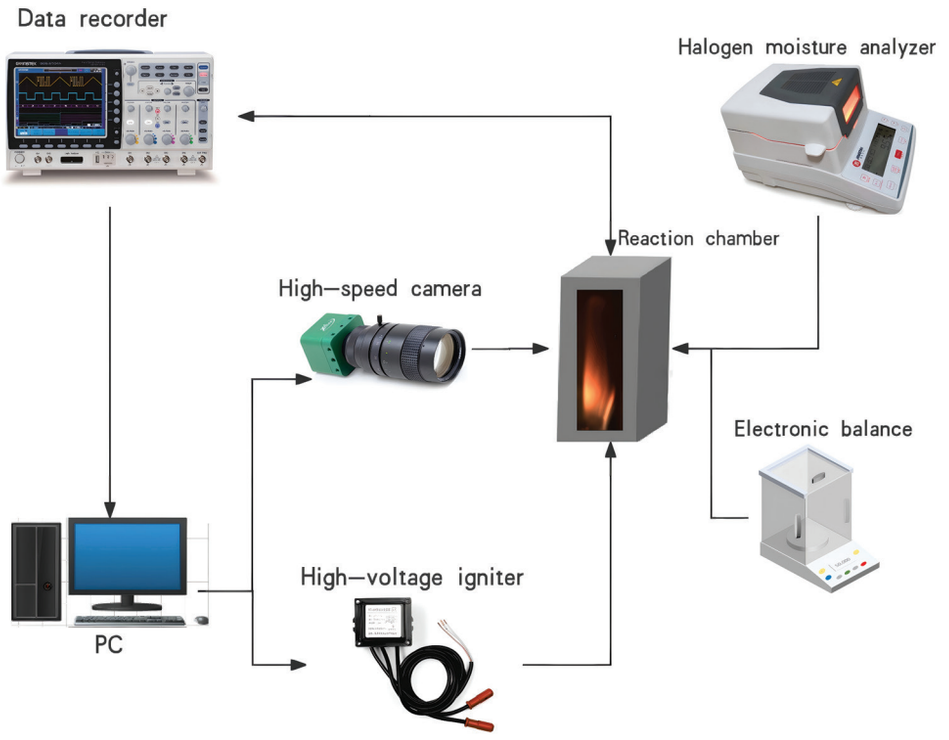

Figure 3. Schematic diagram of the deflagration test apparatus

2.4. Determination of porosity and density parameters

The following parameters were determined to assess porosity and density:

(i) Porosity (ϕ): Porosity is defined as the ratio of pore volume to total volume in a material, calculated as:

$$\phi=V_{pores}/V_{total} \quad (II)$$

Where V_{pores} is the volume of interconnected and isolated voids within the material matrix (including open and closed pores), and V_{total} is the total apparent volume encompassing both solid constituents and void spaces (measured geometrically at standard atmospheric pressure).

(ii) Bulk density (ρ_b): Bulk density is defined as the mass of a material per unit volume, including all internal and interparticle voids. The formula is expressed as:

$$\rho_b=m/V_{total} \quad (III)$$

Where m is the mass of the material (including both solid and porous phases), and V_{total} is the total apparent volume encompassing solid constituents and void spaces.

(iii) True density (ρ_p): True density refers to the mass per unit volume of the solid constituents of a material, excluding all internal pores and interparticle voids. The formula is expressed as:

$$\rho_p=m/V_{solid} \quad (IV)$$

Where m is the mass of the cotton floc, and V_{solid} is the volume of solid constituents excluding all void spaces.

(iv) Porosity-bulk density interconversion: Based on the fundamental definitions of porosity and bulk density, their intrinsic relationship is derived as:

$$\phi=1-\rho_b/\rho_p \quad (V)$$

2.5. Model construction and assumptions

Models are typically used to describe the reaction kinetics and the effects of pore structure on combustion behavior, providing a solid theoretical basis for subsequent experimental verification. The integration of reaction kinetics and diffusion constraints allows for a more accurate prediction of flame propagation characteristics under different structural and environmental conditions.

In the global reaction kinetic model, the corresponding reaction equations are as follows:

$$C_6H_{10}O_5+6O_2\rightarrow 6CO_2+5H_2O \quad (VI)$$

$$\dot{\omega}_{kinetic} = Ae\,\hat{}\,(-\frac{Ea}{RT}) \quad (VII)$$

Where $\dot{\omega}_{kinetic}$ is the chemical reaction rate, governed by the Arrhenius equation; A is the pre-exponential factor, 1.0×10^8 s^{-1}; Ea is the activation energy,

140 kJ/mol; T is the temperature; and R is the universal gas constant, 8.314 mol/K.[39]

In the structure-reaction coupled modification model, the actual reaction rate is limited by diffusion, and can be expressed as:

$$\dot{\omega}_{actual} = \min\left(\dot{\omega}_{kinetic}, \dot{m}_{O_2} \cdot \text{stoichiometric ratio}\right) \quad \text{(VIII)}$$

Where $\dot{m}_{O_2}$ is the maximum oxygen diffusion flux limited by the pore structure characteristics, and the stoichiometric ratio refers to the mass ratio of oxygen to fuel required for complete combustion. When oxygen diffusion capacity is inadequate, the reaction rate is constrained to $\dot{m}_{O_2}$ times the oxygen requirement per unit fuel.

3. Results and discussion

3.1. Physical structure and combustion behavior of elongated fibrous biomass

Biomass materials, such as cotton floc found in northern China, exhibit high combustibility due to their fibrous composition, high porosity, and low-density characteristics. Microscopic analysis of cotton floc (Figure 4) reveals an interwoven, porous fiber network capable of entrapping substantial air. This structure facilitates rapid oxygen diffusion across fiber surfaces, markedly increasing the specific surface area. Consequently, cotton floc exhibits an accelerated combustion reaction rate, leading to enhanced heat release and rapid flame propagation.

In addition, the low density of cotton floc plays a crucial role in its high flammability. A lower density implies a greater air volume per unit mass, enhancing oxygen availability while facilitating rapid heat dissipation during combustion, thereby accelerating flame propagation. Moreover, the fiber surface readily adsorbs water vapor and volatile combustible gases, further increasing its susceptibility to ignition, particularly under elevated temperatures or static charge accumulation.

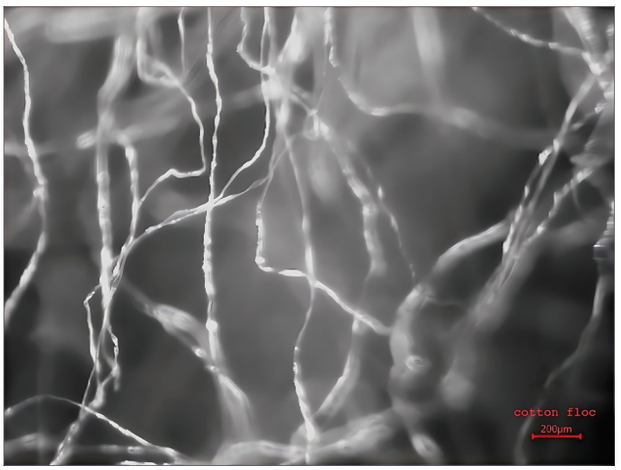

Figure 4. Microscopic structure of cotton floc. Scale bar: 200 μm.

Taken together, the high specific surface area, loose and porous structure, low density, and gas adsorption capacity, coupled with its inherent flammability, render cotton floc highly susceptible to deflagration under certain conditions.

3.2. Deflagration behavior of elongated fibrous biomass

In the deflagration test, 1.3 g of cotton floc was uniformly placed inside the pipeline, with the high-voltage electric spark generator positioned at the bottom. The high-speed camera recorded the position of the flame front over time, and the flame propagation speed was calculated based on the flame front's position at different time points.

In the pipeline experiment, under unsealed conditions, the flame front reached the top cap within 240 ms after ignition of the cotton floc, corresponding to a flame propagation speed of 0.833 m/s in an open environment. Under sealed conditions, the flame front reached the top cap within 130 ms after ignition of the cotton floc, resulting in a flame propagation speed of approximately 1.538 m/s.

Deflagration is defined as a combustion process in which the flame propagation speed remains below the speed of sound in compressible media, typically ranging from several to tens of meters per second. In the sealed pipeline experiment, the observed flame propagation speed of 1.538 m/s aligns with the characteristics of subsonic combustion propagation.

Considering the physical properties of cotton floc and its combustion characteristics, it can be concluded that its combustion is a rapid process that remains subsonic, aligning with the defining features of deflagration. This process is driven by heat release from high-temperature gases and the combustion reaction, propagating the flame front forward, rather than by high-temperature, high-pressure shock waves. The observed average flame propagation speed of 1.538 m/s in the sealed pipeline experiment further confirms that cotton floc undergoes a deflagration reaction under confined conditions.

Based on flame imaging and the combustion products formed, the deflagration process can be classified into the following three stages:[40,41]

(i) Pyrolysis stage in low-density regions (diffusion-dominated combustion): In the initial stage of deflagration, the 3D fibrous network of cotton floc, characterized by high porosity (>80%), forms an open structure where the oxygen diffusion rate exceeds the pyrolysis gas generation rate. The high-temperature electric arc from the spark initiates the thermal decomposition of cellulose and hemicellulose, producing volatile species such as CO and CH_4, which dissipate rapidly through the porous matrix. At this stage, combustion is primarily diffusion-driven, exhibiting progressive surface carbonization (volume shrinkage rate >60%) without visible flames (Figure 5). The high permeability of the fiber network delays combustible gas accumulation, establishing a characteristic "surface pyrolysis-gas diffusion" coupling mode.

(ii) Oxidation stage in critical-density regions (deflagration transition): As pyrolysis progresses, the fibrous network contracts under thermal stress, reducing porosity to a critical range (55 – 65%) and forming a semi-enclosed gas cavity. Within this confined structure, volatile gases accumulate and mix with oxygen, reaching a pre-mixed concentration of 12 – 15%, which falls within the flammability limits, thereby triggering chain radical reactions. This transition marks a combustion mode shift from diffusion-controlled burning to pre-mixed deflagration, characterized by flame propagation speeds of 1.2 – 1.8 m/s and peak temperatures exceeding 800°C. High-speed camera imaging reveals that turbulence effects induced by the critical porosity structure drive a fractal expansion pattern of the flame front (Figure 6).

(iii) Char combustion stage in high-density regions (smoldering-dominated combustion): As the fibrous network undergoes carbonization, its porosity decreases to <40%, leading to severe oxygen diffusion constraints and the formation of a dense char layer. At this stage, combustion transitions into a heterogeneous surface oxidation regime, where the residual char (fixed carbon content >75%) reacts with oxygen through the Knudsen diffusion mechanism, with reaction kinetics dictated by oxygen penetration depth within nanoscale pores (<50 nm). Macroscopically, this stage exhibits smoldering characteristics, with a surface glowing temperature of ~550°C and an ash residue rate exceeding 90%. The process ultimately self-extinguishes due to pore closure, with this smoldering phase persisting 3 – 5 times longer than the initial deflagration stage, underscoring the dominant role of mass transfer limitations in combustion kinetics at high densities (Figure 7).

3.3. Structural fuel theory of cotton floc deflagration

While classical dust deflagration theory adequately describes the fundamental combustion characteristics of cotton floc, its turbulence-mixing-dominated combustion mechanism fails to fully account for experimentally observed anomalies. Under confined conditions, the flame propagation velocity of cotton floc combustion (1.538 m/s) significantly exceeds that in loosely packed configurations (0.833 m/s), with combustion efficiency exhibiting local maxima at specific bulk densities. These findings suggest that cotton floc combustion is not solely governed by turbulent fuel-oxidizer mixing

Figure 5. The pyrolysis stage in the deflagration process of cotton floc

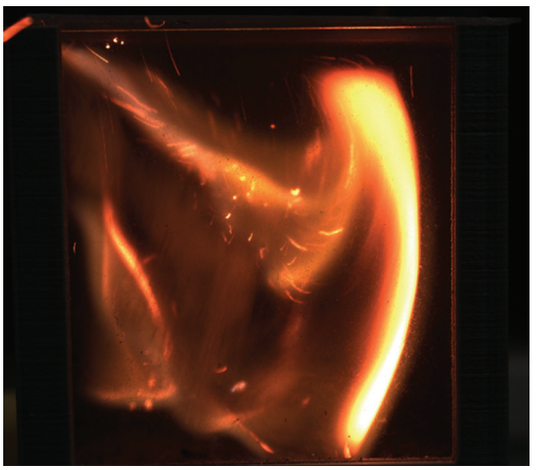

Figure 6. Oxidation stage in the deflagration process of cotton floc

but is instead directly influenced by dynamic porosity evolution within the fibrous network.[42]

By integrating porous media combustion theory[43] with fibrous fuel combustion dynamics,[44] a porosity-governed combustion framework is proposed, wherein 3D fibrous network architectures regulate combustion mode transitions through porosity modulation. This progression shifts from diffusion-controlled combustion in low-density regimes to deflagration in critical-density zones, ultimately reaching oxygen-starved combustion in high-density domains ($\phi < 40\%$). This framework advances the understanding of biomass combustion behavior by elucidating structural-thermochemical coupling mechanisms and provides a foundation for optimizing energy release efficiency in fibrous biofuels through targeted porosity engineering. The differences between conventional dust deflagration and cotton floc deflagration theories are presented in Table 1.

Table 2 presents a comparison between the model-predicted and experimentally measured flame propagation speeds at a porosity (ϕ) of 35%. The predicted speed was 1.48 m/s, while the experimental value was 1.538 m/s, resulting in an error of 3.9%. This close agreement validates the accuracy of the predictive model and supports its applicability for simulating flame behavior under similar conditions.

3.4. Experimental data and analysis

Referring to GB/T 16425-2018, "Dust Cloud Explosion Lower Concentration Determination Method," the experiment commenced with a biomass fuel bulk density of 80 g/m^3, with the subsequent increases in density applied in fixed-step increments. Although this standard is primarily applicable to different types of fuels, it serves as a useful reference framework and methodological guide for this study. The upper explosion limit is typically not considered as a key indicator; rather, it is defined as a certain density, beyond which explosion parameters significantly decrease. Table 3 presents the experimental data on cotton floc, including the input mass and the corresponding reaction time and utilization rate.

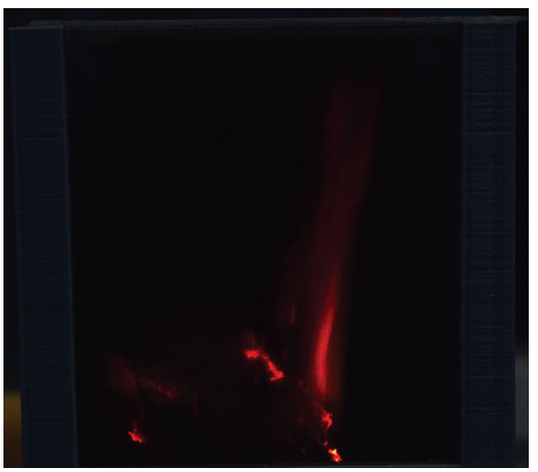

Figure 7. Carbon combustion stage in the deflagration process of cotton floc

Figure 8 illustrates the relationship between cotton floc input mass and the corresponding utilization rate, revealing a distinct trend: as the input mass increases, the utilization rate initially declines sharply before gradually reaching a stable value. This relationship curve can be segmented into several distinct phases:

(i) High utilization phase: At low input mass (*e.g.*, 0.08 g), the utilization rate approaches 1 (95.13%), indicating efficient resource conversion

(ii) Rapid decline phase: As input mass increases to 0.16 and 0.24 g, the utilization rate decreases significantly to 55.88% and 58.17%, respectively

(iii) Gradual slowdown phase: From 0.32 g onward, the decline in utilization rate moderates, but fluctuations become apparent, with notable inflection points around 0.64 g (33.88%) and 0.88 g (16.15%)

Table 1. Comparative analysis between cotton floc deflagration and conventional dust deflagration theories

Property	Conventional dust deflagration	Cotton floc deflagration
Oxidant supply mechanism	Turbulent stochastic mixing	Porosity-guided laminar permeation
Energy release mode	Global homogeneous reaction	Directional combustion wave propagation
Key control parameter	Dust concentration (LEL/UEL)	Fibrous bulk density (porosity, ϕ)
Stabilization approach	Inert gas suppression	Active porosity modulation

Abbreviations: LEL: Lower explosive limit; UEL: Upper explosive limit.

Table 2. Flame propagation speed of model prediction versus experimental value

Output	Model prediction	Experimental value	Error
Flame propagation speed (sealed conditions)	1.48 m/s	1.538 m/s	3.9%

Table 3. Input mass of cotton floc and corresponding measurements

Input mass (g)	Bulk density (g/m^3)	Porosity	Residual mass (g)	Utilization rate (%)	Reaction time (s)
0. 08	80	0. 9481	0. 0039	95. 13	0. 55
0. 16	160	0. 8961	0. 0706	55. 88	0. 49
0. 24	240	0. 8442	0. 1004	58. 17	0. 40
0. 32	320	0. 7922	0. 2068	35. 38	0. 38
0. 40	400	0. 7403	0. 2298	42. 55	0. 39
0. 48	480	0. 6883	0. 3319	30. 85	0. 34
0. 56	560	0. 6364	0. 4128	26. 29	0. 31
0. 64	640	0. 5844	0. 4232	33. 88	0. 32
0. 72	720	0. 5325	0. 5840	18. 89	0. 32
0. 80	800	0. 4805	0. 6292	21. 35	0. 22
0. 88	880	0. 4286	0. 7379	16. 15	0. 37
0. 96	960	0. 3766	0. 7826	18. 48	0. 13
1. 04	1040	0. 3247	0. 8306	20. 13	0. 25

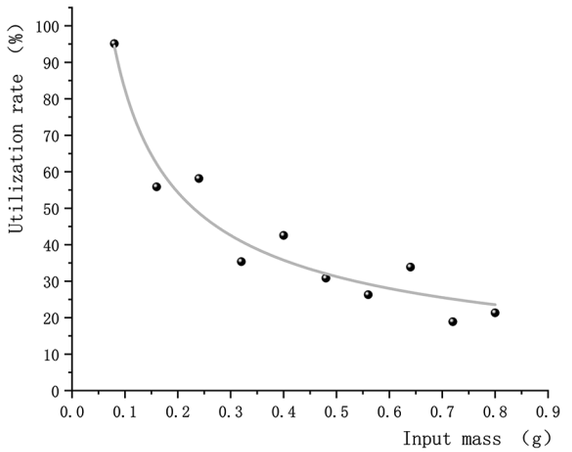

Figure 8. Variation in cotton floc utilization rate as a function of input mass

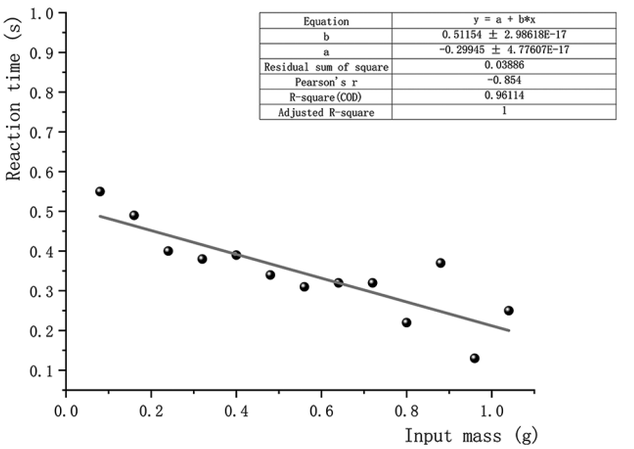

Figure 9. Variation in cotton floc deflagration reaction time as a function of input mass

(iv) Low utilization stabilization phase: At higher input masses (*e.g.*, 1.04 g), the utilization rate stabilizes at a lower level (20.13%).

These findings suggest that increasing input mass reduces resource efficiency, but the rate of decline eventually saturates, leading to a stable but low utilization phase.

Figure 9 displays the variation in reaction time as a function of input mass. The plot/trendline confirms the linearity of the experimental data, providing a theoretical basis for predicting reaction time in practical applications. This approach allows for a more targeted experimental design and operation, optimizing the control of cotton floc explosion and improving reaction efficiency. It can be observed that as the input mass increases, the reaction time generally decreases. When the input mass is small (0.08 – 0.24 g), the reaction time gradually decreases from 0.55 to 0.40 s. As the input mass further increases to 0.4 g, the reaction time briefly increases to 0.39 s, but then steadily declines with further mass increases (up to 0.72 g), reaching a minimum of 0.22 s. At high input mass (0.8 – 1.04 g), the reaction time displayed greater fluctuations, initially increasing to 0.37 s, then sharply decreasing to 0.13 s, and subsequently rising again to 0.25 s. The experimental results reveal that at a cotton floc input mass of 0.64 g, the porosity approaches the critical threshold of 50%, leading to a reduction in reaction time to 0.32 s and a local peak in resource utilization (33.88%). This

porous structure significantly enhances gas-solid mass transfer, facilitating a dynamic equilibrium between oxygen transport capacity and combustion demand. As a result, it sustains combustion stability while maximizing reaction intensity, ultimately achieving an optimized balance between energy density and reaction efficiency. These findings provide key experimental evidence for the parameter optimization of resource-efficient combustion systems.

Pearson correlation analysis was used to study the correlation between residual mass, utilization rate, reaction time, and input mass, with the Pearson correlation coefficient (r) representing the strength of the relationship (Table 4). It was observed that there is a significant positive correlation between residual mass and input mass (r = 0.995). In contrast, the utilization rate and input mass displayed a significant negative correlation (r = −0.852). Similarly, reaction time and input mass exhibited a significant negative correlation as well (r = −0.854). These significant correlations suggest that input mass is an important factor influencing cotton floc deflagration. Reasonable control of input mass can optimize the balance between residual mass, utilization rate, and reaction time, providing guidance for improving resource utilization efficiency and reaction control.

The non-linear trend in resource utilization and the dynamic variation in reaction time with increasing input mass in the cotton floc deflagration experiment result from the interplay of multiple factors. At low input masses, reactants have sufficient oxygen availability, enabling complete combustion and high utilization efficiency. As input mass increases, the accumulation of reactants restricts oxygen diffusion, leading to incomplete combustion and a rapid decline in utilization rate. Concurrently, hindered heat transfer results in localized temperature rises, which may promote side reactions or induce fluctuations in the combustion rate, further reducing resource efficiency. At high input mass, oxygen availability becomes the primary limiting factor, leading to a decrease in reaction rate, prolonged reaction duration, and increased fluctuations. However, at moderate input mass (*e.g.*, 0.64 g), a dynamic equilibrium is established between oxygen supply, heat transfer, and reactant diffusion, enabling a more intense and efficient reaction, with utilization efficiency reaching a local peak. This phenomenon highlights the interdependence of oxygen supply, thermal transport, and material diffusion within the reaction system, underscoring that precise control of input mass is crucial for optimizing reaction efficiency and resource utilization.

Table 4. Correlation analysis between input mass and key parameters

Parameter	Residual mass	Utilization rate	Reaction time
r	0.995	−0.852	−0.854
p	1.39e-10	0.0013	0.0011

Note: Statistical values indicate the correlation (r) and significance (p) of each parameter relative to the input mass.

The pore structure of cotton floc governs flame propagation by forming gas diffusion channels. Predominantly, large pores form continuous pathways that significantly enhance oxygen transport, accelerate convective diffusion of volatile compounds, and promote rapid flame front advancement, especially in confined environments. In contrast, a high proportion of small pores causes local airflow blockages at fiber junctions, restricting oxygen supply and markedly slowing flame spread. Moreover, non-uniform pore distribution intensifies flame front oscillations.

The pore structure of cotton floc regulates reaction time by coupling heat and mass transfer processes. Highly interconnected pore networks enhance radiative heat penetration, markedly reducing fuel preheating duration. A moderate presence of small pores prolongs the residence time of volatiles, promoting thorough oxidation. However, an excessive fraction of small pores can cause localized heat accumulation and oxygen imbalance, potentially disrupting the reaction. Within an optimal porosity range, the synergy between large and small pores maximizes oxygen diffusion and synchronizes heat release, thereby minimizing reaction time, as illustrated in Figure 10.

3.5. Future work and prospects

Precise regulation of porosity enables synergistic improvements in combustion safety, energy efficiency, and emission reduction. Pre-combustion compression of waste cotton flocs to lower porosity helps suppress deflagration chain reactions and improves gas-solid mass transfer. During combustion, staged oxygen-enriched strategies further enhance efficiency and reduce emissions of CO, NO_X, and PM2.5. In addition, establishing porosity safety thresholds within regulatory frameworks, combined with gas monitoring and ventilation systems, facilitates cleaner, more efficient, and controllable biomass utilization.

To further enhance the safety and efficiency of biomass energy utilization, it is recommended that

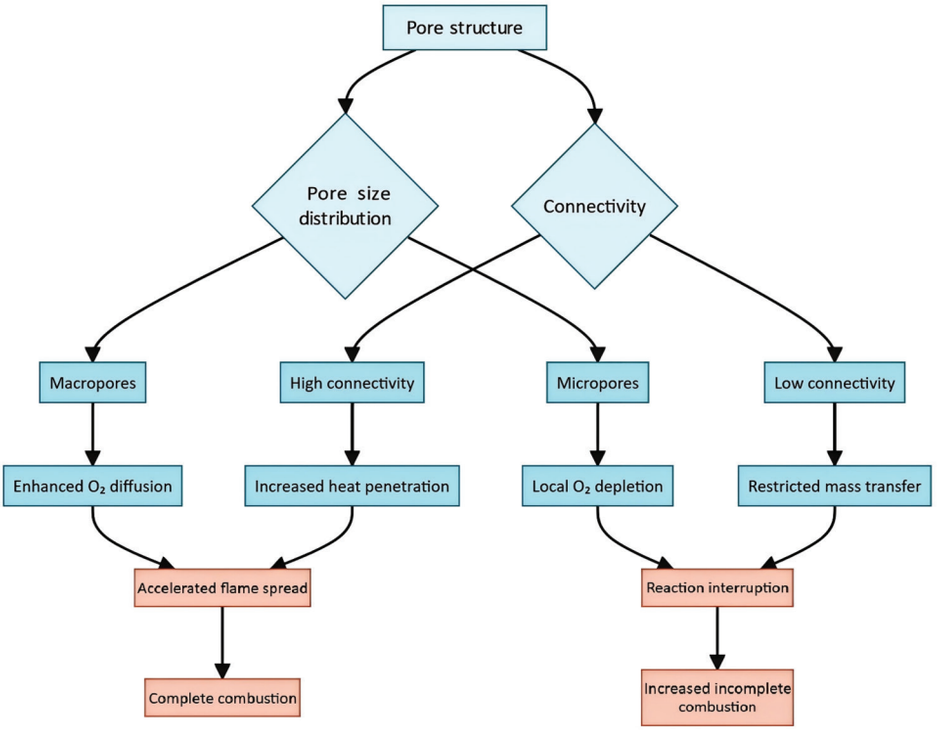

Figure 10. Potential mechanisms of pore structure influencing deflagration

reactor design fully integrate pore dynamics and adaptive load regulation strategies. By implementing staged feeding and optimizing structural configurations, regions with different porosity can be effectively matched to promote thorough volatile release and prolong char residence time, thereby improving overall reaction efficiency and reducing residual losses. Coordinated oxygen concentration control, especially in localized low-porosity areas, can mitigate incomplete combustion and reduce emissions of CO and harmful gases. In addition, combining real-time load adjustments with automated feeding systems ensures that the reactor operates consistently within a high-efficiency combustion range, avoiding efficiency collapse. This comprehensive optimization approach not only enhances energy conversion performance but also minimizes pollutant emissions, supporting cleaner and more stable energy use and providing a robust foundation for future equipment upgrades and process improvements.

To mitigate fire risks during biomass storage and transport, a systematic prevention strategy involving density monitoring, zoned management, and explosion-proof design is essential. Precise monitoring and dynamic adjustment of bulk density and porosity effectively prevent the formation of flammable premixed gases, reducing the risk of deflagration and dust explosions. Zoned stacking strategies combined with humidity control and sprinkler systems help suppress local heat accumulation and self-ignition in both open and enclosed environments. During transport, mechanical compression and inert gas injection further strengthen safety measures. From a policy perspective, strict monitoring protocols and safety standards should be established, including real-time gas detection and ventilation systems to ensure safe operation of storage and transport systems. The integration of rapid online diagnostic and early-warning technologies enables the timely identification and intervention of potential fire hazards, ultimately improving the intrinsic safety of the entire system.

In future work, mixed-level orthogonal experiments will be employed to systematically assess the combined effects of porosity on reaction time, flame propagation speed, and combustion intensity. Displacement sensors will be used to measure deflagration pressure, enabling further refinement of the findings. Although the approach employed in this study has certain limitations, it sufficiently supports the present findings. Future enhancements in experimental design and measurement accuracy will enhance the generalizability and robustness of the results, thereby providing a more

comprehensive understanding of the influence of pore structure on combustion behavior.

5. Conclusion

Based on a comprehensive experimental investigation and data analysis, the key findings of this study are as follows:

(i) Resource utilization: Resource utilization efficiency peaks at low input mass (<0.4 g) but declines sharply beyond this threshold before stabilizing. This trend likely results from oxygen diffusion limitations within pore channels, although confounding factors (*e.g*., airflow turbulence) require further investigation

(ii) Reaction kinetics: Reaction time generally decreases with increasing input mass but exhibits a transient increase at approximately 0.4 g. This anomaly may arise from localized combustion instability caused by pore blockage, necessitating validation against heat transfer delays or microexplosion events

(iii) Optimized combustion regime: Enhanced combustion efficiency (33.88%) and reduced reaction time were observed at 0.64 g input mass and ~50% porosity. This suggests pore-mediated optimization of gas-solid mass transfer, though the "optimum" is dependent on experimental boundaries (*e.g*., confined space, fixed fiber topology)

(iv) Porosity-governed transition: Increasing bulk density drives a combustion shift from diffusion-limited burning to deflagration, ultimately leading to oxygen-starved combustion (<40% porosity), delineating a porosity-dependent regime distinct from fibrous fuels

(v) Environmental impact: Pore structure influences combustion emissions, with low porosity and confined conditions leading to increased CO, NO_X, and PM2.5 outputs. Incomplete pyrolysis and residual char accumulation exacerbate air pollution and associated health risks.

Acknowledgments

The authors are grateful to Beijing Forestry University for the support and resources provided to complete this research; the Biomass Laboratory of Beijing Forestry University for providing advanced facilities and invaluable guidance throughout the study; and professors and colleagues whose ongoing support and constructive feedback significantly enhanced the quality of this work.

Funding

This study was funded by the Beijing Forestry University through a grant awarded to Zhongjia Chen (grant number: 31500478).

Conflict of interest

The authors declare that they have no known competing financial interests or personal relationships that could have influenced the work reported in the article.

Author contributions

Conceptualization: Qingchun Wang
Data curation: Zhongjia Chen
Formal analysis: Zhuoying Chen
Investigation: Zhiyuan Ma
Methodology: Qingchun Wang
Writing – original draft: Zhiyuan Ma
Writing – review & editing: Xiangyue Yua, Zhongjia Chen

Availability of data

All experimental data required to reproduce the findings of this study are included in the article. Raw datasets may be obtained from the corresponding author upon reasonable request.

References

1. Scott V, Haszeldine RS, Tett SF, *et al*. Fossil fuels in a trillion tonne world. *Nat Climate Change*. 2015;5(5):419-423. doi: 10.1038/nclimate2578
2. Sanchez LD, Nelson HJ, Johnston J, *et al*. Biomass enables the transition to a carbon-negative power system across western North America. *Nat Climate Change*. 2015,5(3):230-234. doi: 10.1038/nclimate2488
3. Staples DM, Malina R, Barrett HR. The limits of bioenergy for mitigating global life-cycle greenhouse gas emissions from fossil fuels. *Nat Energy*. 2017;2(2):024001-756. doi: 10.1038/nenergy.2016.202
4. Abouallal H,Idrissi EN, Dkhireche N, *et al*. Biomass as an alternative solution to energy production and reduction of the greenhouse gas emissions: A review. *Int J Power Energy Convers*. 2025,16(1):78-99. doi: 10.1504/IJPEC.2025.142878
5. Ladanai S, Vinterbäck J. Global potential of sustainable biomass for energy. *Sustain Dev Energy Water Environ*

Syst. 2009;7(3):193-203.
6. Sertolli A, Gabnai Z, Lengyel P, Bai A. Biomass potential and utilization in worldwide research trends-A bibliometric analysis. *Sustainability*. 2022;14(9):5515. doi: 10.3390/SU14095515
7. Szklo A, Rochedo P, Schaeffer R. The potential of biomass. In: *Energy Transitions and Climate Change*. United Kingdom: Edward Elgar Publishing; 2023.
8. Erra MR, Dias TA, Maya DM, Lora EE. Global bioenergy potentials projections for 2050. *Biomass Bioenergy*. 2023,170:106721. doi: 10.1016/J.BIOMBIOE.2023.106721
9. Wang JY, Fu JY, Zhao ZT, *et al*. Benefit analysis of multi-approach biomass energy utilization toward carbon neutrality. *Innovation*. 2023;4(3):100423. doi: 10.1016/j.xinn.2023.100423
10. Huang C. *Investigations on Deflagration Characteristics and Inerting Suppression of Combustible Wood-plastic Mixed Dus*. China: Wuhan University of Technology; 2021. doi: 10.27381/d.cnki.gwlgu.2021.000572
11. Zhang B, Zhang Z, Wang J, *et al*. Study of pyrolysis and explosion characteristics of two types of wood fiber. *China Forest Products Industry*. 2024;61(01):20-25. doi: 10.19531/j.issn1001-5299.202401004
12. Jiang B, Xu K, Liu B, *et al*. Experimental study on ignition and explosion characteristics of DDGS dust and thermal reaction analysis. *J Safety Sci Technol.* 2023;19(9):136-142. doi: 10.11731/j.issn.1673-193x.2023.09.020
13. Zhang S, Yu J, Ding J, *et al*. Experimental study on flame propagation and pressure characteristics of corn starch explosion under airflow transport conditions. *CIESC J.* 2024;75(5):2072-2080. doi: 10.11949/0438-1157.20231387
14. Zhang R, Deng Y, Deng H, *et al*. Experimental study on lower limit of tapioca starch explosion. *Blasting*. 2020;37(3):134-140. doi: 10.3963/jissn.1001-487X.2020.03.023
15. Chen J. *Study on the Combustion and Explosion Characteristics of Biomass Pellet Fuel Dust*. China: Guangdong University of Technology; 2021. doi: 10.27029/d.cnki.ggdgu.2021.000281
16. Liu A, Chen J, Huang X, *et al*. Explosion parameters and combustion kinetics of biomass dust. *Bioresour Technol*. 2019;294:122168. doi: 10.1016/j.biortech.2019.122168
17. Lv P, Gu X, Li G, *et al*. Research progress on thermal stability of combustible dust. *China Saf Sci J.* 2023;33(12):92-103. doi: 10.16265/j.cnki.issn1003-3033.2023.12.1228
18. Wang Z, Yang S, Luan W, *et al*. Review on the test of minimum ignition energies of dust clouds. *Sci Technol Eng.* 2023;23(4):1357-1369.
19. Zhang J, Zhou H. Study on minimum ignition temperature of bamboo dust clouds explosion. *Forest Grassland Mach*. 2018;29(5):14-18. doi: 10.13594/j.cnki.mcjgjx.2018.05.005
20. Wu L, Yu L, Wang T, *et al*. Explosion characteristics of oil shale dust in a confined space. *Explos Shock Waves*. 2022;42(1):157-166. doi: 10.11883/bzycj-2021-0139
21. He Y, Li H, Zhu J, *et al*. Experimental study on the ignition and explosion of tobacco dust. *Electr Explosion Protect.* 2023;4:24-27+31. doi: 10.14023/j.cnki.dqfb.2023.04.007
22. Yang J, Zhu D, Xu H, *et al*. Experimental study on explosion characteristics of erythophyll dust. *Indust Saf Environ Protect.* 2015;41(9):24-27.
23. Islas A, Fernández AR, Betegón C. Computational assessment of biomass dust explosions in the 20L sphere. *J Hazard Mater*. 2022;430:130337. doi: 10.1016/J.PSEP.2022.07.029
24. Islas A, Fernández AR, Betegón C. Biomass dust explosions: CFD simulations and venting experiments in a 1 m³ silo. *J Hazard Mater*. 2023;448:130736. doi: 10.1016/J.PSEP.2023.06.074
25. Medina CH, MacCoitir B, Sattar H, Slatter DJ. Comparison of the explosion characteristics and flame speeds of pulverised coals and biomass in the ISO standard 1 m³ dust explosion equipment. *Fuel*. 2015;158:1-9. doi: 10.1016/j.fuel.2015.01.009
26. Slatter DJF, Sattar H, Medina CH. Biomass explosion residue analysis. In: *Proceedings of the International Symposium on Hazardous Materials and Explosions*. Vol. 25. 2014.p. 333-341.
27. Shen F, Xiong X, Fu J, *et al*. Recent advances in mechanochemical production of chemicals and carbon materials from sustainable biomass resources. *Renew Sustain Energy Rev*. 2020;130:109944. doi: 10.1016/j.rser.2020.109944
28. Liu A, Chen J, Lu X, *et al*. Influence of components interaction on pyrolysis and explosion of biomass dust. *Proc Saf Environ Protect*. 2021;154:384-392. doi: 10.1016/J.PSEP.2021.08.032
29. Wen X, Lu C, Shen F, *et al*. Experimental study on unsteady dynamic propagation characteristics of biomass pyrolysis gas/air premixed explosion. *J Safety Environ*. 2024;24(6):2190-2196. doi: 10.13637/j.issn.1009-6094.2023.1377
30. Yang G, Xu Y, Yang R, *et al*. Experimental study on explosiveness of biomass fuel. *Chin J Explos Propellants*. 2024;47:1114-1123. doi: 10.14077/j.issn.1007-7812.202405005
31. Liu X, Li D, Yang J, *et al*. Kinetic mechanisms and emissions investigation of torrefied pine sawdust utilized as solid fuel by isothermal and non-isothermal experiments. *Materials*. 2022;15(23):8650-8650. doi: 10.3390/MA15238650

32. Mulky CT, Niemeyer EK. Computational study of the effects of density, fuel content, and moisture content on smoldering propagation of cellulose and hemicellulose mixtures. *Proc Combust Inst*. 2019;37(3):4091-4098. doi: 10.1016/j.proci.2018.06.164
33. Azam MS, Lukasz N, Yousaf MA, *et al*. Combustion and explosion characteristics of pulverised wood, valorized with mild pyrolysis in pilot scale installation, using the modified ISO 1m^3 dust explosion vessel. *Appl Sci*. 2022,12(24):12928-12928. doi: 10.3390/APP122412928
34. Mularski J, Li J. A review on biomass ignition: Fundamental characteristics, measurements, and predictions. *Fuel*. 2023;340:127526. doi: 10.1016/J.FUEL.2023.127526
35. Li J, Paul CM, Younger LP, *et al*. Prediction of high-temperature rapid combustion behaviour of woody biomass particles. *Fuel*. 2016;165:205-214. doi: 10.1016/j.fuel.2015.10.061
36. Wang Q. *Study on the Methane-Air Deflagration Flames Propagation Characteristics in an Square Plexiglass Tube*. China: University of Science and Technology of China; 2013.
37. Dong Z, Fu B, Chu Y, *et al*. Explosion characteristics of wood dust and its suppression in typical powder-related environments. *Powder Technol.* 2024;435:119389. doi: 10.1016/J.POWTEC.2024.119389
38. Jiang H, Bi M, Li B, *et al*. Combustion behaviours and temperature characteristics in pulverized biomass dust explosions. *Renew Energy*. 2018;122:45-54. doi: 10.1016/j.renene.2018.01.063
39. Liang Y, Ries ME, Hine PJ. Pyrolysis activation energy of cellulosic fibres investigated by a method derived from the first order global model. *Carbohydr Polym*. 2023;305:120518. doi: 10.1016/j.carbpol.2022.120518
40. Lei J, Wang Y, Wang Q, *et al*. Evaluation of kinetic and thermodynamic parameters of pyrolysis and combustion processes for bamboo using thermo gravimetric analysis. *Processes*. 2024;12(11):2458-2458. doi: 10.3390/PR12112458
41. Chen D, Cen K, Zhuang X, *et al*. Insight into biomass pyrolysis mechanism based on cellulose, hemicellulose, and lignin: Evolution of volatiles and kinetics, elucidation of reaction pathways, and characterization of gas, biochar and bio-oil. *Combust Flame*. 2022;242:112142. doi: 10.1016/J.COMBUSTFLAME.2022.112142
42. Wang Q, Liu K, Wang S. Effect of porosity on ignition and burning behavior of cellulose materials. *Fuel*. 2022;322:124158. doi: 10.1016/J.FUEL.2022.124158
43. Bear J. *Dynamics of Fluids in Porous Media*. United States: Courier Corporation; 2013.
44. Drysdale D. *An Introduction to Fire Dynamics*. United States: John Wiley and Sons; 2011.